Acta Cryst. (1962). **15**, 1146

Crystallographic Changes with the Substitution of Aluminum for Iron in Dicalcium Ferrite

By Deane K. Smith*

Portland Cement Association Fellowship, National Bureau of Standards, Washington 25, D.C., U.S.A.

(15 *September* 1961 *and in revised form* 18 *January* 1962)

Single-crystal X-ray precession patterns of several compositions in the solid solution series

$$Ca_8(Fe_{1-p}Al_p)_8O_{20}\ (0 \le p \le 0.69)$$

show that the series is not completely isostructural. Systematic extinctions of X-ray reflections indicate that the space group for compositions with the ratio $p \equiv Al/(Al+Fe)$ less than 0·30 is *Pnma*, whereas the space group for p greater than 0·33 is *Imma*. The cell constants vary continuously throughout the symmetry change.

The crystal structure determined by Bertaut, Blum & Sagnières (1957, 1959) for the iron end-member has the 8 Fe in two 4-fold sites, one site octahedrally coordinated with oxygen and one tetrahedrally coordinated with oxygen. The layers of octahedra correspond to the space group *Imma*, but the layers of tetrahedra reduce the symmetry to *Pnma*. The substitution of Al for Fe in this structure causes the tetrahedral layer to adjust gradually to the *Imma* symmetry.

Steric considerations and relative intensities of $0k0$ reflections for various compositions suggest that the Al atoms substitute preferentially for tetrahedrally-coordinated Fe atoms until about half the tetrahedral cations are Al. Then additional Al distributes itself nearly equally between the tetrahedral and octahedral sites until it saturates the tetrahedral sites at approximately $p = 0.69$, the composition limit for crystallization of this phase from CaO–Fe_2O_3–Al_2O_3 melts.

In the ternary system $CaO–Fe_2O_3–Al_2O_3$ there exists a continuous solid solution from the compound $2CaO.Fe_2O_3$ along the join $2CaO.Fe_2O_3–2CaO.qAl_2O_3$ (q = 1·058) to a composition with the ratio $p \equiv Al/(Al+Fe)$ around 0·69. This solid solution has been the subject of several investigations since Hansen, Brownmiller & Bogue (1928) first found $4CaO.Al_2O_3.Fe_2O_3$, now known as brownmillerite, and showed the existence of a continuous solid solution between it and $2CaO.Fe_2O_3$. Further studies in this system by McMurdie (1937), Yamauchi (1937), Swayze (1946), Malquori & Cirilli (1952), and Newkirk & Thwaite (1958) show that the solid solution composition with the maximum alumina content is approximately $6.5CaO.2.3Al_2O_3.Fe_2O_3$. Toropov & Boikova (1955, 1956) suggest that this composition may be closer to $8CaO.3Al_2O_3.Fe_2O_3$, but other researchers have not verified this extension of the series.

X-ray crystallographic studies of these calcium aluminoferrite solid solutions were first made by Büssem (1937, 1938). They established that the crystals of $4CaO.Al_2O_3.Fe_2O_3$ were orthorhombic with the probable space group *Imma*. Büssem postulated a structure for brownmillerite consisting of tetragonal layers of AlO_6 octahedra alternating with orthorhombic layers of FeO_4 tetrahedra. The calcium ions bond the layers. Cirilli & Burdese (1951) and Malquori & Cirilli (1952) agreed with *Imma* as the probable space group for the entire solid solution series and added support to a structure basically as proposed by Büssem (1938), but with the Al atoms substituted randomly for Fe in both tetrahedral and octahedral sites. The unit-cell formula in either case is $Ca_8(Fe_{1-p}Al_p)_8O_{20}$.

During the first complete determination of the crystal structure of a member of the solid solution series, Bertaut, Blum & Sagnières (1957, 1959) established that the true space group for the $Ca_8Fe_8O_{20}$ end-member is *Pnma*. Their final structure is very similar to the one proposed by Büssem (1937, 1938). Because the X-ray patterns indicating *Pnma* symmetry show weak reflections where absences would occur if the space group were *Imma*, they assumed these weak reflections had been missed in the earlier investigations and that the space group *Pnma* was valid for the solid solution series. Based on this assumption, they list atomic coordinates for brownmillerite with the Al replacing the tetrahedrally coordinated Fe. The present investigation establishes that the space group for brownmillerite is *Imma* while that of $Ca_8Fe_8O_{20}$ is definitely *Pnma*, and, therefore, the two compositions are not completely isostructural.

Malquori & Cirilli (1952) and Midgley (1952, 1957, 1958) have shown by X-ray powder diffraction studies that the unit cell constants vary continuously with composition, and suggest that cell constants as determined by X-ray diffraction be used as a means for determining the Al_2O_3/Fe_2O_3 ratio of the alumino-

---

* Present address: Lawrence Radiation Laboratory, Livermore, California, U.S.A.

ferrite phase in portland cement. This technique is now being used quite successfully (Copeland *et al.*, 1959). Malquori & Cirilli (1952) and Midgley (1952, 1957, 1958)* show graphs for interplanar spacings of powder lines as a function of composition, not all of which are linear. The curves for unit-cell dimensions as a function of composition show in some cases a change of slope around the ratio $p=0{\cdot}33$. Recently, Newkirk & Thwaite (1958) have shown that there is at least a slight change of slope in the curves of all three unit-cell constants at a ratio p very close to 0·33. Hansen, Brownmiller & Bogue (1928) have shown curves of optical indices of refraction plotted with respect to composition with a marked change in curvature around $p=0{\cdot}25$. The birefringence, which is 0·09 at $p=0{\cdot}0$ and 0·07 at $p=0{\cdot}5$, has a minimum of 0·02 at this composition.

X-ray data on the solid solution

As part of an investigation to determine the nature of the aluminum substitution for iron in the solid solution, single crystals of several compositions were grown from melts. About 0·2 g. of material of the desired composition was sealed in a platinum capsule. Several of these capsules were hung in a vertical tube furnace and cooled at the rate of one degree per day, starting above the liquidus temperature. When the temperature fell below the solidus, the capsules were removed from the furnace. Prismatic crystals up to $1\times1\times2$ mm. in size were obtained. Sharp peaks in the X-ray powder patterns of the crystallized materials indicate that no significant compositional zoning is present. Thus it may be assumed that the composition of individual crystals is the same as the bulk composition of the materials from which they were grown.

Powder diffraction patterns using diffractometer techniques were made of all the samples using a single lot of Ag powder as the internal standard. Fig. 1 shows the variations with composition of the unit cell dimensions and the interplanar spacings of two important lines. The 141 spacing and the a axis (as determined from the 200 line) show linear relationships.

The b axis (from 080) changes continuously but with a distinct change in slope around $p=0{\cdot}33$ as mentioned previously. The c axis (from 002) and the 202 spacing show non-linear changes also, with a curvature opposite to that found for the b axis.

X-ray precession patterns of the $hk0$, $h0l$, and $0kl$ zones were obtained with Zr-filtered Mo $K\alpha$ radiation ($\lambda=0{\cdot}711$ Å) from single crystals with $p=0{\cdot}00$, 0·06, 0·26, 0·30, 0·33, 0·50, and 0·67. Crystals with a ratio p equal to and greater than 0·33 showed the systematic absences $hk0$ when $h=2n+1$ or $k=2n+1$, $h0l$ when $h+l=2n+1$, and $0kl$ when $k+l=2n+1$. Upper level patterns verify that extinctions occur for hkl when $h+k+l=2n+1$. These extinctions are characteristic of the space group *Imma* or *Im*2*a*. Crystals with p less than 0·33 showed only the extinctions $hk0$ when $h=2n+1$ and $0kl$ when $k+l=2n+1$, corresponding to the space group *Pnma* or *Pn*2₁*a*. As p increases

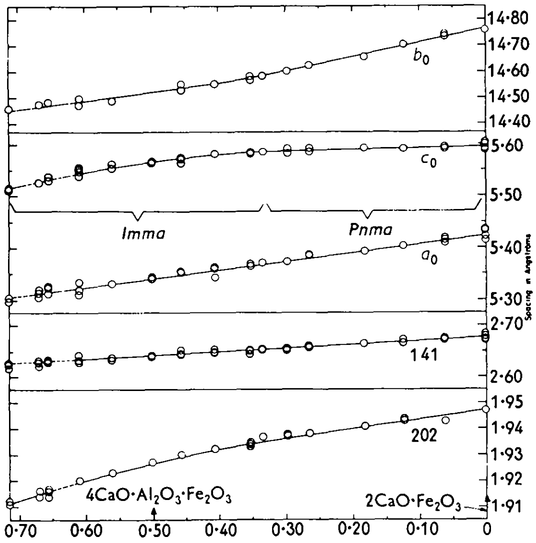

Fig. 1. Variation of cell constants and interplanar spacings with composition. The lines drawn for 141 and 202 are calculated from the a_0, b_0, and c_0 curves. The dotted portion indicates the sample used showed slight traces of a second phase.

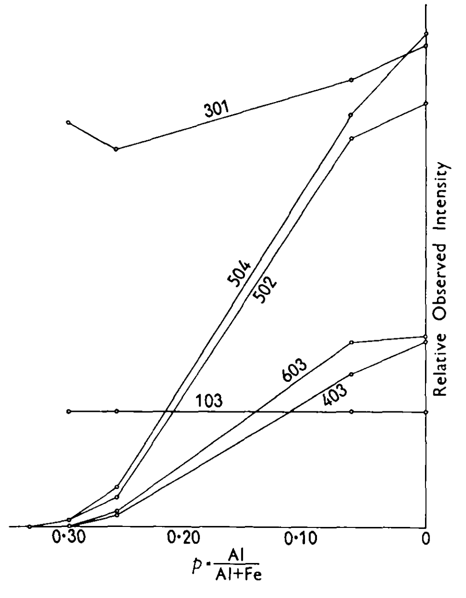

Fig. 2. The decrease of intensity for $h0l$ reflections with $h+l=2n+1$ with increasing Al content. The reflection 103 is used as a reference.

---

* Malquori & Cirilli (1952) and Midgley (1952, 1957, 1958) have erroneously indexed the strongest line of the powder diffraction patterns as 200 instead of 141. Indexed patterns for $Ca_8Fe_8O_{20}$ and the brown millerite composition are given by Bertaut, Blum & Sagnières (1959) with the exception that they have interchanged the a and c axes from the usual orientation. An indexed pattern of $Ca_8Fe_8O_{20}$ is given in the Appendix.

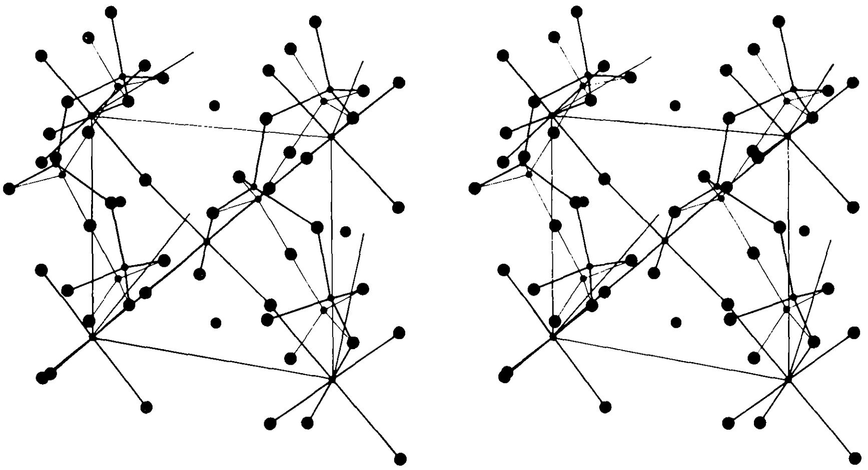

Fig. 3. Stereoscopic pair showing half the unit cell in the structure of $Ca_8Fe_8O_{20}$ as determined by Bertaut, Blum & Sagnières (1959) viewed approximately along the *b* axis. The atoms connected by the lighter lines indicate the proposed structural change when $p \geq 0{\cdot}33$. The partial outline of the unit cell is shown; the *a* axis is vertical, the *b* axis is toward the back of the drawing, and the *c* axis slopes down to the right. The Fe and Al sites are shown as small circles, the oxygen sites as large circles, and the Ca sites as intermediate size circles without bonds.

from zero to 0·33, the relative intensities of the reflections permitted by *Pnma* or $Pn2_1a$ but forbidden by *Imma* or *Im*2*a* (*hk*0, $k=2n+1$; *h*0*l*, $h+l=2n+1$) decrease with respect to the other intensities in the respective zones. Fig. 2 illustrates graphically the change of relative intensities (measured by simple photometry of the precession patterns) for several reflections in the *h*0*l* zone, using the intensity of (103) as reference because its intensity is about the same as the observed reflections with $h+l=2n+1$. The composition range in which the space group changes corresponds with the change in slope of the unit-cell constants shown in Fig. 1.

Because the composition of the solid solution in equilibrium with a melt changes with temperature, compositional zoning in the crystals might be expected. Such zoning, if present, would produce X-ray patterns with the spots markedly elongated because of the variation of unit cell with changing composition. The reflections most affected would be those at high angles. For precession patterns the relative change in spacing *D*, for a given relative change in the distance *r* from the center of the pattern to the corresponding reflection is

$$dD/D = -dr/r\ .$$

For a crystal with $p=0{\cdot}33$ the diameter of the 0·20·0 spot is about 0·3 mm., approximately the same as for all other reflections on the pattern. For this reflection $r=58{\cdot}5$ mm. Assuming that the spot may be elongated 0·1 mm.

$$dD/D = -0{\cdot}0017\ .$$

Thus the *b* axis may vary by an amount which, according to Fig. 1, corresponds to a compositional change of 5 mol.%. Thus even if this much elongation is present, the composition variable *p* departs from the average no more than ±2·5% within the crystal.

The actual change of space group in this solid solution series is not discontinuous. The cell constants vary continuously with composition, and the intensities of sensitive reflections, in Fig. 2, approach extinction with a slope that is either zero or slightly positive at the phase change. From the present data it is not possible to state precisely the value of *p* at which this phase change occurs, but this value is apparently between 0·30 and 0·33.

Structural changes with composition

The crystal structure determined by Bertaut, Blum & Sagnières (1957, 1959) for the iron end-member is shown as a stereoscopic pair in Fig. 3. It consists of a network of layers of FeO_6 octahedra alternating with layers of FeO_4 tetrahedra with the Ca atoms located interstitially between the layers. The latter layers consist of infinite chains of tetrahedra running parallel on the average to the *a* axis but somewhat buckled in the *ac* plane by compression along the chain direction. The octahedral layers have the *Imma* symmetry; it is slight deviations from the ideal *Imma* positions in the tetrahedral layer and for the Ca positions, which reduce the symmetry to *Pnma*. Thus the substitution of Al for Fe must cause structural changes in the tetrahedral layer.

In the $Ca_8Fe_8O_{20}$ structure the 8Fe atoms are in two 4-fold positions, the 8Ca atoms in the general 8-fold position, and the 20 oxygen atoms in two 8-fold positions and one 4-fold position. Table 1 gives the atomic coordinates as determined by Bertaut, Blum & Sagnières. The only other composition in the series which is rigorously assignable to these positions is brownmillerite, in which 4Al could occupy one of the 4-fold Fe positions. Other compositions would require either some type of superlattice or a statistical distribution of the substituting ions. No evidence was found on any of the X-ray patterns for a superlattice in any of the solid solutions. Crystals of all other compositions must therefore have a statistical distribution of the Fe and Al atoms. Table 2 shows the *Pnma* positions and the most logical corresponding *Imma* positions and coordinates as given in the *International Tables for X-ray Crystallography* (1952).

Table 1. *Atomic coordinates for the* $Ca_8Fe_8O_{20}$ *end-member as determined by Bertaut, Blum & Sagnières* (1959)

	x	y	z
Fe_I in 4(*a*)	0·000	0·000	0·000
Fe_{II} in 4(*c*)	−0·055	0·250	−0·072
Ca in 8(*d*)	0·480	0·112	0·028
O_I in 8(*d*)	0·250	−0·015	0·250
O_{II} in 8(*d*)	0·000	0·133	0·055
O_{III} in 4(*c*)	0·607	0·250	−0·137

Table 2. *Probable corresponding equivalent positions for the atoms in the space groups Pnma and Imma*

	Pnma Al/(Al + Fe) < 0·33	*Imma* Al/(Al + Fe) > 0·30
Fe_I	4(*a*)	4(*a*)
Fe_{II}(Al)	4(*c*)	4(*e*)
Ca	8(*d*)	8(*h*)
O_I	8(*d*)	8(*g*)
O_{II}	8(*d*)	8(*h*)
O_{III}	4(*c*)	4(*d*)

Several possibilities exist for the Al substitution. The Al atoms may replace the Fe atoms randomly, or they may substitute in the octahedral or tetrahedral sites preferentially. Because the substitution must particularly affect the tetrahedral layer, the random substitution is considered unlikely, as it would cause the structure to shrink uniformly with little reason for a symmetry change. If the Al replaced the octahedrally-coordinated Fe, the octahedral layer should contract, and the shortening of the *a* repeat distance would cause the tetrahedral chains to buckle even more than they already have. Again no symmetry change would take place. However, if the tetrahedral Fe is replaced by Al, the tetrahedra will shrink with respect to the octahedral layer, and the chain can straighten to produce the higher *Imma* symmetry. The non-linearity of the optical constants with respect to composition also supports the belief that random substitution is unlikely.

The relationship of the two structures is shown in the stereoscopic pair in Fig. 3. The environment of oxygen atoms around the Ca becomes more symmetrical and the Ca atoms shifts onto the newly created mirror plane. The Fe_{II} position must shift by 0·30 Å, the O_{III} by 0·58 Å, and the Ca by 0·11 Å.

The ratio of Al to Fe at the change of space groups is approximately one to three. If all the Al is in the tetrahedral sites, the ratio of tetrahedral Al to tetrahedral Fe is one to one. The Al might be expected to occupy alternate sites along the chain since this configuration might lead to a low potential energy. Such a regular distribution would change the crystal symmetry to *Pmmb* or *Imm*2, neither of which is allowed by the observed X-ray reflections. Because the allowable non-centrosymmetric space group, *Im*2*a*, cannot be developed from the Bertaut structure by systematic substitution of Al, it appears that the space group should be the centrosymmetric *Imma*. If the chains consisted of short portions of alternating Fe and Al tetrahedra occasionally shifted in phase by mistakes in the order, or if well-ordered individual chains were randomly placed with respect to each other, the short range order would not be detected in the present study.

Further support for the preferential Al substitution in the tetrahedral layers may be found in the relative intensities of the 0*k*0 reflections. These reflections are not affected by the x and z coordinates of the atoms, and if the postulated structural changes are correct, the y coordinates will not be changed significantly. Hence, the 0*k*0 intensities are functions of the relative amounts of Al and Fe. Fig. 4 represents the intensities for the 0*k*0 reflections assuming the Al replaces the tetrahedral Fe until all tetrahedral sites are substituted. The reflections with $k = 4n$ are insensitive to distribution of Al since the contribution from both sites is positive, and a continuous decrease in absolute intensity occurs with increasing Al content.

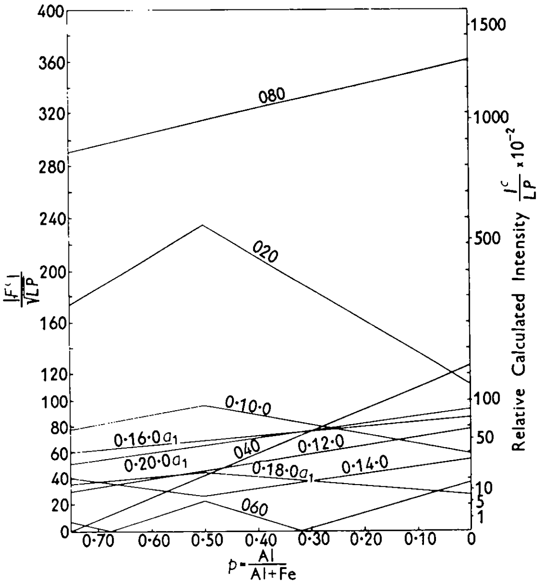

Fig. 4. Calculated intensities for 0*k*0 reflections assuming the Al substitution is tetrahedral for $p < 0.5$ and octahedral for $p > 0.5$.

The intensities of the 0*k*0 reflections with $k = 4n + 2$ are sensitive to the distribution of the Al and Fe atoms because the structure amplitudes of the two sites are opposite in sign. For the reflections 020, 0·10·0, and 0·18·0 the structure factor is positive and increases if the Al goes into tetrahedral sites. Octahedral substitution on the other hand would cause a decrease in these intensities. The structure factors for 060 and 0·14·0 are both negative for the iron end-member; therefore, their intensities would decrease with tetrahedral substitution or increase with octahedral substitution. The 060 intensity is so low that the sign of its structure factor eventually reverses. Substitution of equal amounts of Al in both tetrahedral and octahedral sites would cause no change in the intensities of the $0k0$ reflections with $k = 4n+2$.

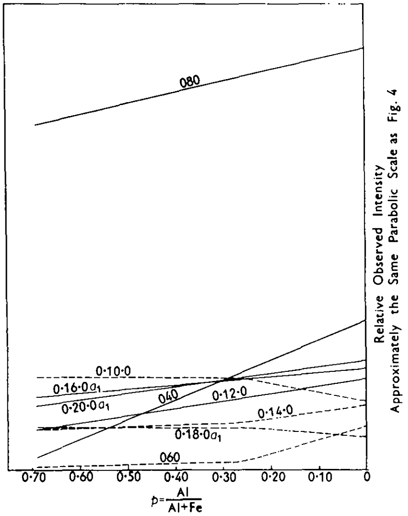

Fig. 5. Approximate observed intensities for $0k0$ reflections. The intensities were estimated by order of magnitude, but not measured by means of a scale.

The estimated relative intensity variations with composition are shown in Fig. 5. The relative intensity changes for low Al content appear to follow the curves for purely tetrahedral substitution. With increasing Al content the curves deviate from the preferential substitution curves, and for p greater than about 0·3 they suggest a nearly equal distribution between the two sites. Most indicative of this change to equal substitution is the relationship of 0·14·0 to 0·18·0. These two intensities approach each other in magnitude but do not become equal until the ratio p is greater than 0·5.

The relative intensities of the $0k0$ reflections with $k = 4n+2$ suggest that the first Al substitutes preferentially for the tetrahedrally coordinated Fe. As this site approaches half saturation, an increasing proportion of the Al apparently substitutes for the octahedral Fe. Around the composition corresponding to the phase change, the number of Al atoms entering the octahedral sites is nearly the same as the number entering tetrahedral sites. The nearly horizontal but slightly converging lines for the 0·14·0 and 0·18·0 intensities in Fig. 5 indicates that the tetrahedral sites are still slightly preferred by the Al. The Al limit of the solid solution may correspond to the composition at which the tetrahedral sites become saturated with Al. Any further addition of Al would have to go completely into the octahedral sites, which may produce an unstable structure and thus limit the solid solution.

If the Al substitution does follow the above pattern, the Fe and Al atoms for the composition referred to as brownmillerite, $Ca_8Fe_4Al_4O_{20}$, are not distributed in separate crystallographic sites. Approximately one-fourth of the octahedral sites and three-fourths of the tetrahedral sites should contain Al. Swayze (1946) determined the solidus–liquidus phase relations for the solid solution and showed that the brownmillerite composition melts over a range in temperature with a change in composition of the solid phase. Although a composition within the solid solution range near brownmillerite acts as a distinct phase in the ternary system $CaO–Al_2O_3–Fe_2O_3$, the specific composition $4CaO.Al_2O_3.Fe_2O_3$ probably is not a definite compound.

Conclusions

In summary the important results of this investigation are:

1. The solid solution $Ca_8(Fe_{1-p}Al_p)_8O_{20} (0 \leq p \leq 0{\cdot}69)$ is not isostructural throughout the entire composition range.
2. The end-member $Ca_8Fe_8O_{20}$ has the space group *Pnma*. The solid solution exhibits a higher-order phase change to the space group *Imma* when the ratio $p \equiv Al/(Al+Fe)$ increases beyond 0·33.
3. The Al atoms substitute in the tetrahedral sites first. The tetrahedra contract with respect to the octahedral layer, and rotate into a position that conforms to *Imma* symmetry. The rotation of tetrahedra also results in a shift of the Ca atoms to conform with *Imma* symmetry.
4. Any Al atoms substituting into the structure with p greater than 0·33 are distributed nearly equally between the octahedral and tetrahedral sites.
5. The composition $4CaO.Al_2O_3.Fe_2O_3$ is not a distinct compound. The Al atoms are substituting for about one-fourth of the octahedrally-coordinated Fe and about three-fourths of the tetrahedrally-coordinated Fe.

APPENDIX

Indexing of the powder pattern of $Ca_8Fe_8O_{20}$

To resolve the confusion in the literature on the indexing of the X-ray powder patterns for the compositions $Ca_8(Fe_{1-p}Al_p)_8O_{20}$, the pattern of the $Ca_8Fe_8O_{20}$ end-member is given in Table 3, indexed on the basis

Table 3. *Measured and calculated spacings for* $Ca_8Fe_8O_{20}$

Space group *Pnma*

		This paper		Midgley (1957)	
Indices	*d*(calculated)	*d*(measured)	*I*(peak height)	*d*(measured)	*I*(peak height)
020	7·380 Å	7·418 Å	10	7·36 Å	4
011	5·233	5·242	4	5·23	1
101	3·896	3·898	10	3·88	2
031	3·695	3·696	24	3·68	4
040	3·690				
131	3·054	3·056	8	3·05	2
002	2·798	2·799	63	2·78	7
200	2·714	2·714	48	2·71	6
141	2·679	2·680	100	2·67	10
051	2·610	2·609	14	2·60	2
060	2·460	2·456	3		
112	2·452				
122	2·357	2·356	5	2·35	1
151	2·352				
231	2·187	2·189	9	2·20	1
240	2·186			2·18	3
161	2·080	2·082	23	2·07	5
202	1·948	1·949	42	1·94	7
152	1·902	1·903	4	1·90	1
222	1·884	1·884	8	1·88	2
251	1·882				
062	1·847	1·847	22	1·84	4
080	1·845				
033	1·744	1·746	9	1·74	3
181	1·667	1·669	5	1·66	1
270	1·665				
252	1·626	1·626	7	1·62	2
331	1·625				
172	1·608	1·609	3		
143	1·592	1·593	15	1·59	4
053	1·577	1·578	6		
341	1·560	1·561	18	1·55	4
082	1·540	1·541	8	1·54	1
262	1·527	1·527	10	1·52	2
280	1·526				
322	1·488	1·488	5	1·48	1
351	1·487				
233	1·467	1·468	7	1·46	1
163	1·434	1·434	5	1·43	1
272	1·431				
361	1·410	1·411	7		
004	1·399	1·400	2		
1,10,1	1·380	1·381	2	1·38	1
024	1·375	1·375	4		
253	1·363	1·364	3		
400	1·357	1·357	4	1·36	1
352	1·351	1·350	2		
410	1·351				
114	1·349				
282	1·340	1·341	10	1·34	4

of the unit cell discussed in this paper. The spacings of all lines permitted by the space group were calculated. Those corresponding to the observed lines are compared in the table with values reported by Midgley (1957) and the diffractometer measurements of the author.

The author would like to thank Dr Fred Ordway for his many helpful discussions during this work. Thanks are also due to Mr Michael Grasso and Mr Robert Thwaite for the preparation of the mixes used in this investigation and the collection of data for Fig. 1.

References

BERTAUT, E. F., BLUM, P. & SAGNIÈRES, A. (1957). *C. R. Acad. Sci., Paris*, **244**, 2944.

BERTAUT, E. F., BLUM, P. & SAGNIÈRES, A. (1959). *Acta Cryst.* **12**, 149.

BÜSSEM, W. (1937). *Fortschr. Min.* **22**, 31.

BÜSSEM, W. (1938). *Proc. Symposium on the Chemistry of Cement*, p. 153. Stockholm.

CIRILLI, V. & BURDESE, A. (1951). *Ric. sci.* **21**, 1185.

COPELAND, L. E., BRUNAUER, S., KANTRO, D. L., SCHULTZ, E. G. & WEISE, C. H. (1959). *Anal. Chem.* **31**, 1521.

HANSEN, W. C., BROWNMILLER, L. T. & BOGUE, R. H. (1928). *J. Amer. Chem. Soc.* **50**, 396.

International Tables for X-ray Crystallography (1952). Vol. I. Birmingham: Kynoch Press.
McMurdie, H. F. (1937). *J. Res. Nat. Bur. Stand.* **18**, 475. (R. P. 987.)
Malquori, G. L. & Cirilli, V. (1952). *Proc. International Symposium on the Chemistry of Cement*, p. 120. London.
Midgley, H. G. (1952). *Proc. International Symposium on the Chemistry of Cement*, p. 140. London.
Midgley, H. G. (1957). *Mag. Concrete Res.* **9**, 17.
Midgley, H. G. (1958). *Mag. Concrete Res.* **10**, 13.
Newkirk, T. F. & Thwaite, R. D. (1958). *J. Res. Nat. Bur. Stand.* **61**, 233. (R. P. 2900.)
Swayze, M. A. (1946). *Amer. J. Sci.* **244**, 65.
Toropov, N. A. & Boikova, A. I. (1955). *Bull. Acad. Sci. U.S.S.R. Div. Chem. Sci.*, p. 887.
Toropov, N. A. & Boikova, A. I. (1956). *Z. neorg. khimii*, **1**, 2106.
Yamauchi, T. (1937). *J. Japan. Ceram. Soc.* **45**, 880.

Acta Cryst. (1962). **15**, 1152

Structure of Mesomorphic Phases

By A. J. Mabis

The Procter & Gamble Company, Miami Valley Laboratories, Cincinnati 39, Ohio, U.S.A.

(*Received* 10 *July* 1961)

The classification scheme of Hermann (1931) for mesomorphic phases has been extended by illustrations of the possible structures in both real and reciprocal space. The X-ray diffraction patterns most likely to be obtained for monochromatic radiation are also illustrated, for both 'powder' and 'single-crystal' type specimens. By comparing observed diffraction patterns of mesomorphic phases with those predicted, it is possible, in some cases at least, to identify the structure type. Several examples of surfactant–water compositions illustrate some of the unusual diffraction patterns that are obtained, and the use of such information to indicate the structure of the phase.

Introduction

Mesomorphic or liquid-crystalline phases are observed for a number of asymmetrically shaped molecules. Classical examples include molecules like ammonium oleate, *p*-azoxyanisole, and polymeric tungstic acid (Brown & Shaw, 1957). Of more practical importance are the mesomorphic phases observed with surfactants, polymers, lipids (e.g. triglycerides), and other biological systems. The study of the structure of such phases is facilitated by a scheme for descriptive classification. Hermann (1931) proposed a classification which does not appear to have received much attention, although Bernal & Fankuchen (1941) refer to the scheme in their plant virus work. By the application of group theory and several assumptions, Hermann derived eighteen structures between classical amorphous at one end of the scale and a well ordered three-dimensional crystal at the other end. It is the purpose of this paper to amplify Hermann's description, particularly with the use of illustrations, to point out the diffraction patterns to be expected, and to show some examples of mesomorphic phases whose diffraction patterns have unique features explained by this classification scheme.

Assumptions and definitions

The reader is referred to Hermann's original description for the details of his derivation. Several translation operations are defined there, which are means of bringing into congruence 'statistically, translationally equivalent' molecules or units of structure. The translation operations are briefly summarized here, with Hermann's symbols retained.

A 'statistical' translation, symbol S, is one in which the ends of the translation vectors fill space with uniform density. The translation from molecule to molecule in a gas is an example.

A 'reciprocal' translation, symbol R, is one for which the locus of the ends of the translation vectors is a set of parallel equally spaced planes.

In a 'direct' translation, symbol D, the equivalent structural units are equally spaced along parallel straight lines.

'Pseudo-direct' translations, symbols P_2, P_1, and P_0, are also defined, which are D-translations with two, one or zero degrees of freedom allowed for the directions of the D-translation. The subscripts indicate the number of degrees of freedom.

These translation types are taken in groups of three, one each for three independent directions in space, to derive possible structures. Not every possible combination of the nine symbols leads to a unique structure. Some combinations are redundant, and may be omitted. Four assumptions (Hermann, 1931), based on logical physical behavior of molecules, allow the rejection of several additional combinations. The four assumptions are: